Enrichment induces structural changes and recovery from nonspatial memory deficits in CA1 NMDAR1-knockout mice

Claire Rampon, Ya-Ping Tang, Joe Goodhouse, Eiji Shimizu, Maureen Kyin and Joe Z. Tsien

Department of Molecular Biology, Princeton University, Washington Road, Princeton, New Jersey 08540-1014, USA

The first two authors contributed equally to this work.

Correspondence should be addressed to J.Z.T. (jtsien@molbio.princeton.edu)

We produced CA1-specific NMDA receptor 1 subunit-knockout (CA1-KO) mice to determine the NMDA receptor dependence of nonspatial memory formation and of experience-induced structural plasticity in the CA1 region. CA1-KO mice were profoundly impaired in object recognition, olfactory discrimination and contextual fear memories. Surprisingly, these deficits could be rescued by enriching experience. Using stereological electron microscopy, we found that enrichment induced an increase of the synapse density in the CA1 region in knockouts as well as control littermates. Therefore, our data indicate that CA1 NMDA receptor activity is critical in hippocampus-dependent nonspatial memory, but is not essential for experience-induced synaptic structural changes.

Comparative anatomical studies of hippocampal cytoarchitecture reveal a selective expansion of the CA1 region in the hippocampus in primates with respect to rodents and in humans with respect to monkeys, suggesting that this subregion is important in human hippocampal function[1]. Damage to the hippocampus or the CA1 subregion in humans leads to deficits in memories of people, objects, places and events ('declarative memory')[2–4]. Similar spatial and nonspatial memory deficits are also observed in a variety of laboratory animals with hippocampal lesions[4,5]. Recordings of neuronal activity in the CA1 subregion of rodents during behavioral tests show the importance of this subregion in the encoding of nonspatial information[6]. However, the molecular mechanisms underlying these processes remain unknown.

N-methyl-D-aspartate (NMDA) receptors are widely distributed in the brain[7] and are essential for the induction of major forms of long-term potentiation (LTP) and long-term depression (LTD)[8,9]. Enhanced NMDA receptor function in the forebrain improves learning and memory[10], indicating its crucial role in these processes. Using the Cre/loxP-mediated recombination system, we developed a region-specific gene-knockout technique to generate conditional-knockout mice in which NMDAR1, a key subunit of NMDA receptor, was selectively deleted in the CA1 subregion[11]. These CA1-specific NMDAR1 knockout mice lacked NMDA-mediated currents and plasticity in the CA1 region and were profoundly impaired in spatial memory tasks[12,13].

In this study, our first goal was to examine the role of CA1 NMDA receptor activity in the formation of nonspatial memory and the effects of enriched experience on these memory functions. Our second goal was to examine whether enriched experience during adulthood could lead to structural changes in the CA1 region, and whether CA1 NMDA receptor-mediated responses are required for such structural modifications. Synaptic structural changes are assumed to be the anatomical substrate of long-term storage of learned experience[14,15]. For example, numbers of dendritic spines in the hippocampus increase after spatial learning in adult rats[16]. Based on findings of NMDA receptor function in the developing brain[17,18], it is postulated that NMDA receptors might be required for behavioral experience-induced structural plasticity in adult brain. However, new dendritic spines can form on mature hippocampal neurons *in vitro* in the absence of synaptic activity[19], and LTP has no effect on synapse number in the CA1 region[20]. These findings imply that the role of the NMDA receptor in structural changes in adult brain might differ from that in the developing brain. By using unbiased stereological electron microscopy, we examined the structural changes in our CA1-KO mice before and after enriched experience.

Results

NMDAR1 knockout in the CA1 region

We confirmed the complete deletion of the NMDAR1 gene in CA1-KO mice using *in-situ* hybridization histochemistry. No NMDAR1 mRNA was detected in the CA1 subregion (**Fig. 1**), indicating that the genetic deletion of NMDAR1 in young adult mice was heritable after three years of breeding and was complete.

Nonspatial learning and memory deficits

CA1-KO and control mice used in all behavioral tests were 2–4 month-old littermates. We used three hippocampus-dependent behavioral tasks to assess associative, nonspatial memory functions. The hippocampus is important in the formation of recognition memory in both human patients and animals [3–5]. However, little is known about its anatomical basis and its molecular and cellular mechanisms[21]. We evaluated recognition memory with a novel-object recognition-memory task[10]. During the training session, the total amount of time spent exploring two objects was 28.62 ± 3.94 seconds in control mice ($n = 17$) and 34.71 ± 3.56 seconds in CA1-KO mice ($n = 12$), and no significant exploratory preference was found between control and CA1-KO mice (data not shown). These observations indicate that these two types of mice have the same levels of motivation, curiosity, and interest in exploring novel objects.

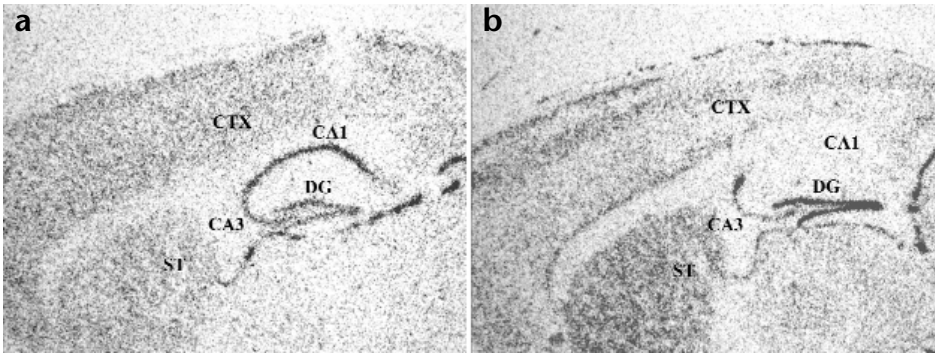

Fig. 1. Cre/loxP-mediated deletion of NR1 gene in CA1-KO mice (2.5 months old) is complete. An antisense 42-mer oligonucleotide recognizing the NR1 gene was used for *in situ* hybridization. CTX, cortex; ST, striatum; DG, dentate gyrus.

For retention tests, at 30 minutes, 2 hours and 24 hours after the training (**Fig. 2**), one object was replaced by a novel object. As expected, control mice showed a significant preference for exploring the novel object during each retention test. In contrast, CA1-KO mice showed only marginal preference for the novel object (**Fig. 2**). A self-ANOVA between training and retention tests revealed a significant difference in control mice ($F_{3,64} = 7.744$, $p < 0.001$) but not in CA1-KO mice. Repeated measures of ANOVA on retention tests showed a highly significant difference between control and CA1-KO mice ($F_{2,27} = 19.435$, $p < 0.001$). A *post-hoc* analysis using Dunnett's test demonstrated significance of this difference in retention at 30 minutes, 2 hours and 24 hours ($p < 0.05$, $p < 0.01$ and $p < 0.01$, respectively; **Fig. 2**). These results indicate profound deficits in novel object recognition memory in CA1-KO.

We then examined olfactory discrimination memory using social transmission of food preference[22]. Rodents develop a preference for foods they have recently smelled on the breath of other individuals[23]. Lesions restricted to the hippocampus impair this kind of memory 24 hours after social interaction (training)[24]. However, the molecular mechanisms underlying this kind of memory remain unknown[22,24]. The task used here consisted of three stages. First, animals became accustomed to eating from a food cup placed on the cage floor. Second, in training sessions, observer mice were allowed to interact with demonstrator mice fed with either cinnamon-scented (1% per weight) or cocoa-scented (2% per weight) food. Third, observer mice were then tested by presentation of both scented foods, and consumption of each food was recorded. Control mice showed a significantly higher preference for food smelled during the training session over unsmelled food than did CA1-KO mice ($F_{1,26} = 5.291$; **Fig. 3**), indicating that olfactory-discrimination memory was impaired in CA1-KO mice. To ensure that this observation was not due to a difference in feeding behaviors, we measured the total amount of food taken during the retention session; this quantity did not significantly differ between control and CA1-KO mice (1.723 ± 0.248 g versus 1.584 ± 0.378 g, respectively). Because these two types of scented food were counterbalanced throughout the experiments, these results indicated that the deficits observed in CA1-KO mice were due neither to abnormal food intake nor to a scent bias *per se*.

We then examined nonspatial memory using a contextual fear-conditioning task[10]. In this hippocampus-dependent task[25], animals learn to fear an environment by associating it with an aversive stimulus (foot shock). Control and CA1-KO mice significantly differed in contextual freezing, but not in freezing responses immediately after the shocks, in retention tests at 2 hours and 24 hours ($p < 0.05$, $p < 0.01$, respectively; **Fig. 4a**), indicating that CA1-KO mice were impaired in contextual fear memory. However, in a cued-conditioning test, which is hippocampus independent[25], freezing responses of CA1-KO mice to a tone were similar to those of control mice in retention tests at 2 hours (data not shown) and 24 hours (**Fig. 4b**). In addition, no abnormal nociceptive responses were found in CA1-KO mice: current required to elicit flinching/running, jumping or vocalization in the CA1-KO mice was the same as in control mice (data not shown). These data clearly showed that hippocampus-dependent, but not hippocampus-independent, fear memory was impaired in CA1-KO mice.

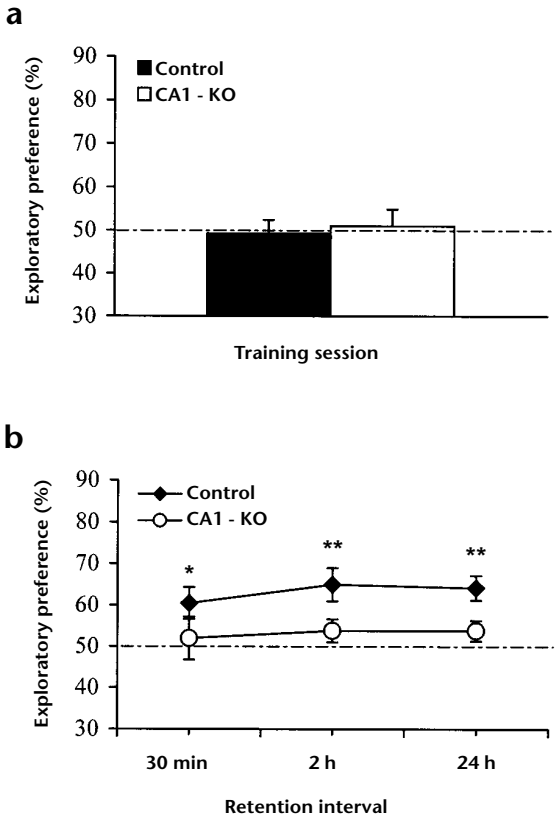

Fig. 2. Impaired novel-object recognition memory in CA1-KO mice. Recognition memory is expressed in terms of exploratory preference in the retention tests. The memory for control (n = 17) or CA1-KO (n = 12) mice was measured at three different time intervals after training. The data are expressed as mean ± s.e.; *$p < 0.05$, **$p < 0.01$, determined by *post-hoc* analysis. We observed similar results in separate groups of CA1-KO and control mice.

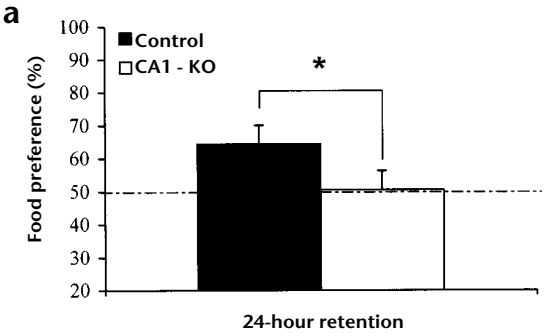

Fig. 3. Social transmission of food preference. Olfaction-discrimination memory is expressed in terms of food preference. (**a**) The memory of either control (n = 15) or CA1-KO (n = 13) mice was measured 24 h after training. (**b**) Food consumption data are expressed as mean ± s.e. *p < 0.05 determined by one-way ANOVA.

Enrichment-induced recovery of memory deficits

These results indicated a profound deficit in three forms of nonspatial memory in CA1-KO mice. Enriched experience can significantly improve performance in spatial maze tests in normal animals[26] and attenuate memory deficits in animals with hippocampal lesions[27]. However, it is not known whether enriched experience can enhance performance of the animals in the three nonspatial memory tasks we used, nor if it is able to rescue the memory deficits observed in CA1-KO mice.

To address these issues, we evaluated nonspatial memory using the same tasks with additional groups of adult animals after they were trained daily in an enriched environment for two months. In the novel-object recognition task, we observed an increase in preference for exploring novel objects in both control and CA1-KO mice (n = 14; n = 12, respectively; **Fig. 5a**). A self-ANOVA between training and retention tests revealed significant differences for control ($F_{3,52}$ = 24.771, p < 0.001) and CA1-KO mice ($F_{3,44}$ = 3.797, p < 0.05), indicating that training in the enriched-environment not only enhanced the performance of normal mice but also attenuated the deficits in CA1-KO mice. An integrated statistical analysis of animals with the same genotype confirmed the effects of training on memory in control mice ($F_{1,29}$ = 7.674, p < 0.05) and in CA1-KO mice ($F_{1,22}$ = 6.674, p < 0.05). However, a repeated measures ANOVA on retention tests still revealed a highly significant group difference between enriched control and enriched CA1-KO mice ($F_{2,24}$ = 11.619, p < 0.01), indicating that enriching experience could only partially rescue the deficits observed in the CA1-KO mice.

In the test of social transmission of food preference, we found that enriched control animals (n = 15) did not increase food preference more than naive animals. This possibly reflected either a ceiling effect or a delicate balance between choosing the preferred food and eating any food after 24 hours of food deprivation. However, food preference of enriched CA1-KO mice (n = 12) was dramatically increased over that of naive CA1-KO animals ($F_{1,22}$ = 4.746, p < 0.05, **Fig. 5b**), indicating that the enriched experience completely rescued the memory deficits in the CA1-KO mice.

We also observed that the enrichment training significantly enhanced contextual freezing in control mice ($F_{1,25}$ = 7.366, p < 0.05) and completely rescued the deficits observed in the CA1-KO mice ($F_{1,23}$ = 14.559, p < 0.001). No significant difference was found between enriched control and enriched CA1-KO mice (**Fig. 5c**). In addition, cued freezing also dramatically increased following enriched experience in both control ($F_{1,25}$ = 6.213, p < 0.05) and CA1-KO mice ($F_{1,23}$ = 4.372, p < 0.001; **Fig. 5d**). These results clearly indicate that the enriched experience could enhance these two kinds of fear memory in control animals and could rescue the deficits in CA1-KO mice.

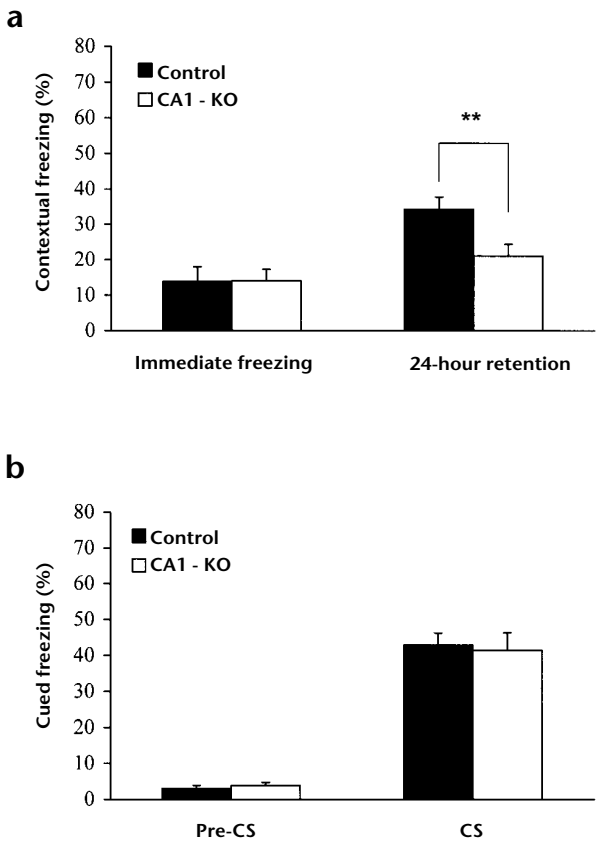

Fig. 4. Fear-conditioning tasks. (**a**) Contextual fear conditioning. Memory is expressed as percent of freezing responses. Immediate learning indicates the freezing response during the 30 s immediately after shock in the training session. Contextual fear memory in controls (n = 14) and CA1-KO (n = 12) was measured 24 h after training. (**b**) Cued fear conditioning. Memory is expressed as percentage of freezing responses. There was no significant difference in proportion of freezing responses either at pre-CS or retention test between control mice (n = 14) and the CA1-KO mice (n = 12). All data are expressed as mean ± s.e., **p < 0.01, determined by one-way ANOVA. Similar results were obtained from another set of experiments.

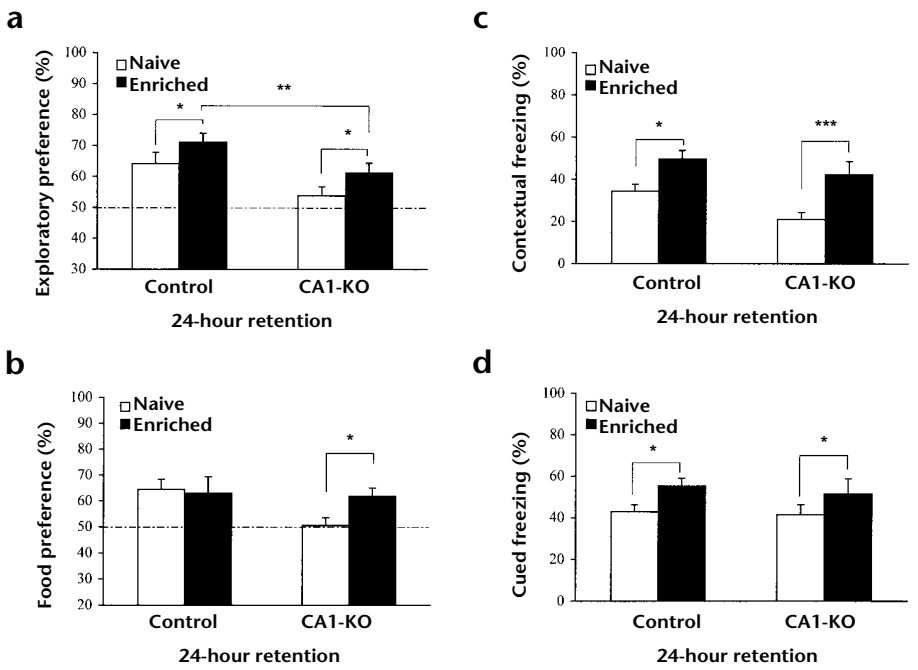

Fig. 5. Effects of enriched experience on nonspatial memory in both control and CA1-KO mice. (**a**) Enriched experience increased exploratory preference in both control (n = 14) and CA1-KO (n = 12) mice in the novel-object recognition task. (**b**) Enriched experience rescued memory deficits of CA1-KO (n = 12) mice in the social transmission of food preference. For control mice, n = 15. (**c**) Enriched experience enhanced contextual freezing response in both control (n = 13) and CA1-KO (n = 11) mice in the fear-conditioning task. There was no significant difference in immediate freezing between the two groups (data not shown). (**d**) Enriched experience increased cued freezing in the fear-conditioning task. There was no significant difference in pre-CS freezing or cued freezing between control mice (n = 13) and CA1-KO (n = 11) mice. All data are expressed as mean ± s.e. *p < 0.05, ** p < 0.01, ***p < 0.001 in one-way ANOVA.

Enrichment-induced anatomical changes

What are the molecular and structural mechanisms underlying the enrichment-induced effects? Enriched experience promotes various biochemical and morphological changes in several brain regions[26,28–31]. Synaptic structural changes are believed to be the anatomical substrate of long-term storage of learned experience, and it is assumed that NMDA receptors are required for experience-dependent anatomical changes in the adult brain. As the first step toward the genetic dissection of the molecular mechanisms of experience-induced structural plasticity in the adult hippocampal CA1 region, we used light and electron microscopy to examine the effects of enrichment on anatomical changes in the CA1 region and the role of the NMDA receptor in this effect.

Nissl-stained tissue of CA1-KO mice shows no gross anatomical abnormality[12]. We used the Golgi-impregnation technique[32] to initially assess dendritic structures. Golgi-impregnated CA1 pyramidal neurons of control and CA1-KO naive animals presented similar dendritic morphology (**Fig. 6a** and **b**). Quantitative analysis of dendritic-spine density on CA1 pyramidal cells revealed no significant difference between naive control (8.1 ± 0.8 spines per 10 μm of apical dendrite, mean ± s.e.) and naive CA1-KO mice (8.6 ± 0.6 spines; **Fig. 6c**). This suggests that conditional knockout of the NMDAR1 gene in the CA1 region, which occurs in the postnatal third and fourth weeks, did not result in abnormal spine density.

To characterize the effects of enrichment on dendritic spine density, we then counted the number of spines on dendrites of CA1 pyramidal cells of enriched animals. We observed a significantly higher density of dendritic spines in enriched contol mice compared with naive animals (10.8 ± 1.1 versus 8.1 ± 0.8; p < 0.05; **Fig. 6c**). This is consistent with a previous report of increased spine density on CA1 neurons in rats after enrichment[16]. Surprisingly, enrichment similarly increased spine density in CA1-KO mice (10.0 ± 0.3 versus 8.6 ± 0.6; p < 0.05). Statistical analysis revealed no significant difference between enriched contol and enriched CA1-KO animals (**Fig. 6c**).

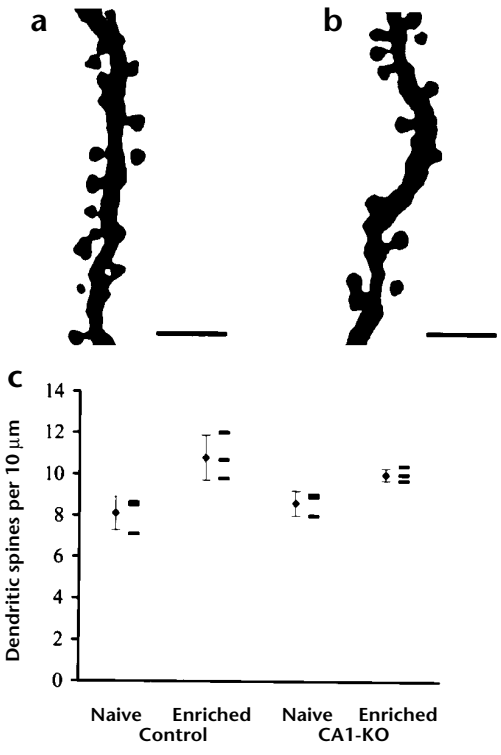

Fig. 6. Enrichment-induced increase in CA1 spine density in both normal control and CA1-KO mice. Photomicrographs of Golgi-impregnated apical dendritic segments of CA1 pyramidal neurons of naive control (**a**) and naive CA1-KO (**b**) mice. (**c**) Bars represent a scatter plot of individual average numbers of dendritic spines per 10 μm length of CA1 pyramidal dendritic segments. Diamonds represent group means ± s.e. (n = 3 for each group). The sexes (M or F) and ages in months of animals in each column (from top to bottom) are naive normal control (M, 3.5; M, 4; M, 3.5), enriched normal control (M, 3.5; M, 5; M, 4.5), naive CA1-KO (M, 4.5; M, 5; M, 4) and enriched CA1-KO (M, 5; M, 5; M, 4.5). *p < 0.05, Mann-Whitney U-test.

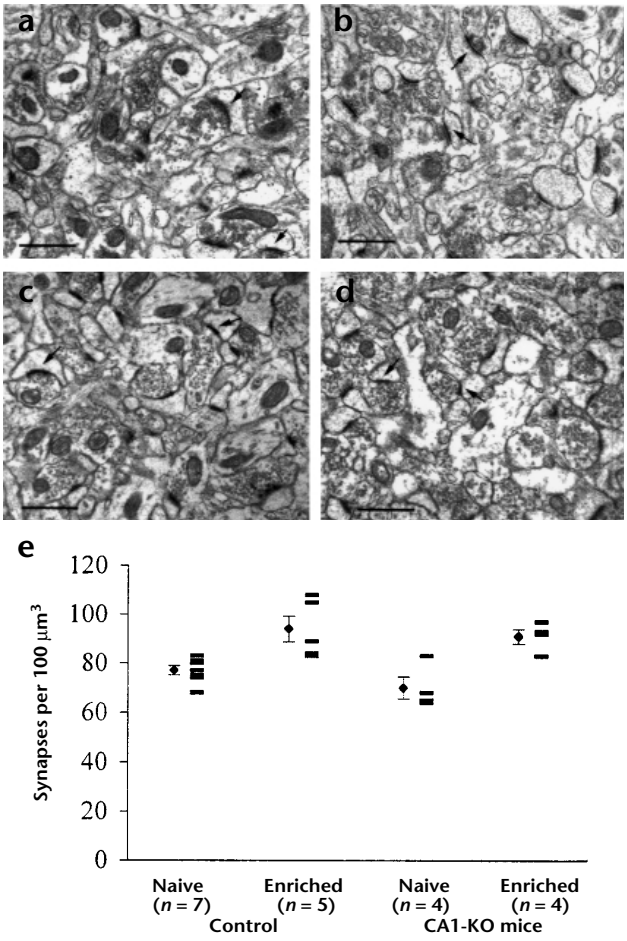

Fig. 7. Enrichment-induced increase in CA1 synapse density in both control and CA1-KO mice. Representative electron photomicrographs illustrating synapses (indicated by arrows) in the stratum radiatum of the CA1 region of naive controls (**a**), naive CA1-KO mice (**b**), enriched controls (**c**) and enriched CA1-KO mice (**d**). Scale bars, 1 μm. (**e**) Diamonds represent group means ± s.e. of estimated synaptic densities in the stratum radiatum of the CA1 region before and after enrichment, calculated with the stereological disector. Bars represent a scatter plot of the CA1 synaptic density in individual animals in each group. The sexes (M or F) and ages in months of animals in each column are (from top to bottom) naive control (M, 4.5; M, 5; M, 4; M, 4; M, 3; M, 3.5; M, 4), enriched control (M, 4.5; M, 5; M, 5.5; M, 4; M, 5), naive CA1-KO (M, 4; M, 4.5; F, 3.5; M, 4) and enriched CA1-KO (M, 3.5; F, 4; M, 4.5; M, 5). *$p < 0.05$, determined by Mann-Whitney *U*-test.

These data indicate that enriched experience resulted in changes in dendritic-spine density and suggest that this increase in spine density can occur in the absence of NMDA receptor activity. These results are consistent with the finding that mature CA1 pyramidal neurons *in vitro* can grow spines in absence of NMDA-receptor activation[19]. However, Golgi staining should be interpreted cautiously. First, this method does not reveal spines hidden beneath or sitting above the dendritic segment, thus, spine density measured this way probably underestimates the actual number of spines. Second, some branched spine heads receive no innervation[33]; therefore, spine density should not be simply extrapolated to synapse density.

To address these concerns, we used electron microscopy to quantitatively analyze synapse density in the stratum radiatum of the CA1 hippocampal region (**Fig. 7a–d**). We ensured unbiased sampling by using the stereological disector technique[34,35]. No significant difference in synaptic density was observed between naive control mice (76.9 ± 1.9 synapses per 100 μm^3, mean ± s.e.) and naive CA1-KO mice (70.0 ± 4.4 synapses, **Fig. 7e**). However, after the enrichment training, control animals showed a significant increase of CA1 synaptic density (93.8 ± 5.3) over the naive control group ($p < 0.05$). Synaptic density was also strikingly higher in trained CA1-KO mice (91.2 ± 2.9) compared to the naive CA1-KO group ($p < 0.01$, **Fig. 7e**). Furthermore, no significant difference in synaptic density was found between enriched control and enriched CA1-KO mice. These data indicate that enriched experience promotes synaptic structural changes in the CA1 hippocampal region. Furthermore, these results suggest that the NMDA receptor is not required for the increase of CA1 synaptic density.

To investigate the possible differential effect of enrichment and NMDA receptor activity on changes in the density of synaptic subtypes, we examined the distribution of CA1 synapses in three major subclasses (non-perforated, perforated and shaft synapses) categorized according to the profile of the postsynaptic density (PSD) in pairs of serial sections. The PSD was classified as non-perforated if the thickening was continuous or as perforated if the PSD was interrupted by electron-lucent regions (**Fig. 8a**). Synapses with asymmetric PSDs on dendritic shafts were identified using Gray's criteria[36]

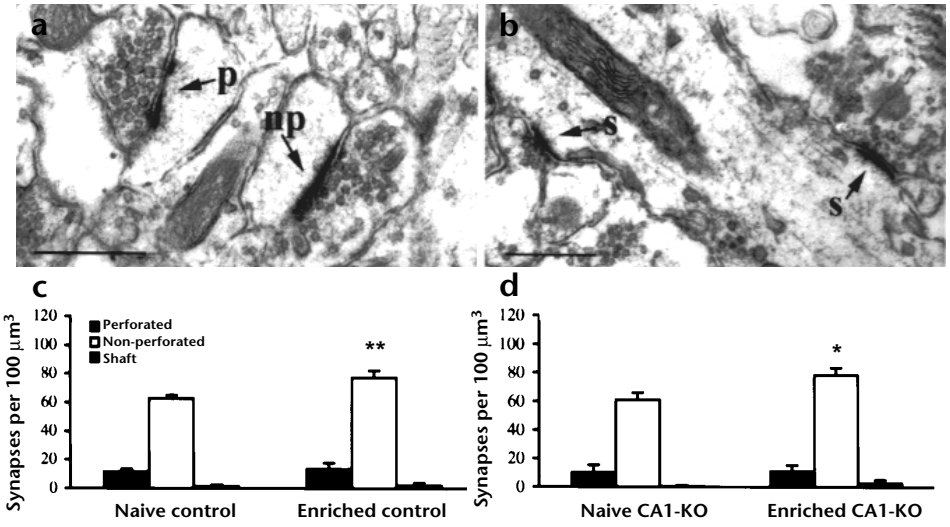

Fig. 8. Major subclasses of CA1 synapses in the CA1 region. (**a**, **b**) Electron micrographs illustrating the ultrastructure of different types of synapses in the stratum radiatum of CA1. Scale bars, 0.5 μm. (**a**) Non-perforated axospinous synapse (np) and perforated axospinous synapse (p). (**b**) Axodendritic synapses involving dendritic shafts (s). (**c**, **d**) Estimated distribution of CA1 synapses in the categories described above for control (**c**) and CA1-KO (**d**) animals, either naive or reared in an enriched environment. Synaptic densities were calculated per surface area and then expressed as the number of synapses per 100 μm^3 by using the stereological coefficient obtained with the disector method. The data are expressed as mean ± s.e.; *$p < 0.05$, Mann-Whitney *U*-test.

and were counted separately from those on dendritic spines (**Fig. 8b**). We found a significantly higher density of non-perforated synapses in control mice after enrichment (77.1 ± 5.2, mean ± s.e.) than in naive control animals (62.6 ± 2.3, $p < 0.05$; **Fig. 8c**). Remarkably, enrichment also significantly increased the density of non-perforated synapses in CA1-KO mice (78.3 ± 5.4 versus 60.7 ± 5.1; $p < 0.05$; **Fig. 8d**), whereas the densities of perforated and shaft synapses remained unchanged after enrichment in both control and CA1-KO mice. For better observation of the synaptic structural changes, a sophisticated approach using three-dimensional reconstruction of synapses viewed through serial electron micrographs would be valuable[33].

Possible tissue shrinkage during the embedding process can be ruled out as explanation for these findings. First, the effect is synapse specific. If there were a generalized shrinkage in the enriched animals with no other change, then all types of synapses should be affected uniformly. Second, the mitochondrial cross-sectional diameters were uniform across the naive and enriched conditions, showing that no generalized shrinkage of individual process occurred (data not shown).

Discussion

Here we examined three kinds of nonspatial memory in mice lacking NMDAR1 in the CA1 region. Our analysis provides evidence supporting the important role of NMDA receptor activity in the CA1 region for the formation of hippocampus-dependent nonspatial memory. Taking into account the deficit in spatial learning in the CA1-KO mice[12], we conclude that NMDA receptor activity in CA1 is essential for the formation of both spatial and nonspatial memory.

More interestingly, we found that the memory deficits associated with the disruption of the hippocampal NMDA receptor could be rescued by daily training in an enriched environment. We show that behavioral experience can enhance learning and memory in the mutant animals. Thus, the memory deficits observed in gentic mutant animals are not necessarily irreversible, and enriched experience could promote recovery of some of the deficits.

To investigate further the possible cellular mechanisms underlying these enrichment effects, we systematically evaluated the anatomical changes using light and electron microscopy. We showed that enriched experience promotes a significant increase in synapse density in the CA1 hippocampal field. Because there is no neurogenesis in the CA1 region[26], the increased synapse density is likely to reflect a higher number of synapses per neuron rather than an increased number of pyramidal cells in CA1. At the ultrastructural level, we showed that mice lacking the NMDA receptor in the CA1 region also increase synaptic density following exposure to an enriched environment. This suggests that NMDA-receptor activity is not required for structural plasticity in the CA1 region of adult animals induced by behavioral experience, and thus the molecular mechanism underlying adult activity-dependent structural plasticity is very different from mechanisms active in the developing brain[17,18]. As synaptic plasticity can also be induced in the CA1 region by an NMDA receptor-independent process[37,38] such as LTP dependent on voltage-gated calcium channels, other mechanisms might serve as putative candidates for experience-induced structural plasticity in adult brain.

It remains to be determined whether the enrichment-induced increase in CA1 synaptic density has any functional role in the concomitant behavioral effects. It is likely that other brain regions may undergo similar biochemical and structural changes after enrichment, and also might participate in the enrichment-induced behavioral improvement. Enhanced synaptic coincidence detection in the forebrain of transgenic mice via upregulation of subunit 2B of the NMDA receptor also leads to overall enhancement of learning and memory[10]. Thus, changes in the composition (for instance, ratio of NR2A to NR2B subunits) of the NMDA receptor complex may be a possible mechanism for the enrichment-induced effects. Taken together, these findings indicate that learning and memory might be enhanced in mammals by genetic factors as well as behavioral experience.

Methods

Animals. The CA1-KO and control mice were produced as described[11]. Throughout the behavioral and histological experiments, observers were blind to the genotype of an individual animal.

***In situ* hybridization.** Described procedures[10] were used. Briefly, an antisense 42-mer oligonucleotide probe (5′-ACC ACT CTT TCT ATC CTG CAG GTT CTT CCT CCA CAC GTT-3′), which recognizes NR1 exon 20, was end labeled with [^{35}S]-dATP. After hybridizing with the oligonucleotide probe (5×10^5 cpm per slide) at 47°C for 24 h, brain sections (20 μm) were washed in 2× SSC at room temperature (RT) followed by two washes in 0.2× SSC at 60°C and one wash in 0.1× SSC at RT. Interestingly, preliminary observations indicated that the deletion of the NR1 gene in six-month-old knockouts seemed to spread to other forebrain regions such as the cortex, probably reflecting the recombination threshold effect as the CaMKII promoter-driven Cre accumulated.

Enriched environment training. Adult littermates (1.5–2 months old) were randomly distributed into two experimental groups. One group was kept in standard cages (naive group) and the other group trained in an enriched environment for three hours daily for two months (enriched group). The enrichment training was carried out in specially designed boxes (1.5 m × 0.8 m × 0.8 m), in which various toys, running wheels and small houses were changed every other day to encourage exploration. Food and water were also available in the boxes. Because electrophysiological, behavioral and anatomical experiments showed similar results for wild-type and Cre transgenic mice, these two genotypes of mice were pooled together as controls.

Novel-object recognition task and fear-conditioning tasks. The experimental protocol was the same as described previously[10], except that the duration of the training period in the object-recognition task was 15 min.

Social transmission of food preference task. In this experiment, 'observer' mice were tested for memory and 'demonstrator' wild-type mice were used to interact with observers according to a described procedure[22]. After interaction, the observers were deprived of food for ~24 h and then tested for memory. During testing, observers were offered both cinnamon- and cocoa-scented food for 2 h, and consumption of each food was subsequently measured. The preferred food had the same scent as food eaten by the demonstrator with whom the observer interacted. Preference was calculated as percentage ratio of the amount of preferred food consumed over 50% of the total amount of food consumed.

Histology. For electron microscopy, contol groups were composed of males, 3.5–5.5 months old. The CA1-KO naive mice were 3 males (4.5, 4 and 4 months) and 1 female (3.5 months), and the CA1-KO enriched mice were 3 males (5, 4.5 and 3.5 months) and 1 female (4 months). Because CA1 dendritic spine density in rats fluctuates over the estrous cycle[39], females were killed during proestrus, the stage at which the spine numbers of female rats approach those of male rats (although it is not known whether the same phenomenon exists in mice). Animals were anesthetized and perfused with 2% paraformaldehyde, 2% glutaraldehyde and 1.5% saturated picric acid in 0.1 M phosphate buffer (pH 7.4) and postfixed overnight in the same solution. Following a modified version of the single-section Golgi impregnation technique[32], 100 μm-thick coronal sections were cut with a vibratome into a bath of 3% potassium dichromate in distilled water and incubated overnight in this solution. The slide assemblies were incubated in the dark in a solution of 1.5% silver nitrate for 2 days.

For electron microscopy, we used a vibratome to cut 250 μm-thick coronal sections into a bath of 0.1 M sodium cacodylate buffer. Hippocampal

sections corresponding to figures 47–50 of the mouse brain atlas[40] were dissected, rinsed in distilled water and postfixed in 1% osmium tetroxide followed with 1% ferrocyanide-reduced osmium tetroxide. Tissues were rinsed, stained *en bloc* overnight in 1% aqueous uranyl acetate, rinsed and dehydrated and subsequently infiltrated and flat embedded with Embed 812 resin. Sections (0.5 μm) were cut and stained with 1% toluidine blue. Sections were examined to determine how the block should be trimmed for ultrathin sectioning to include the apex of the CA1 pyramidal cell layer, from the stratum radiatum to the stratum lacunosum moleculare. Ultrathin sections were cut with a diamond knife, placed on carbon Formvar-coated slot grids and stained with 1% uranyl acetate and lead citrate. Section thickness was measured by scanning electron microscope measurements to range from 0.087 to 0.105 μm, depending on the series.

Data analysis: spine density. Golgi-impregnated dendritic segments selected for analysis were located 100–250 μm from the pyramidal cell bodies in the stratum radiatum, belonged to a thoroughly impregnated pyramidal neuron, remained approximately in the plane of focus and were >10 μm in length and 0.80–1 μm in width. Calculations of spine density were obtained by measuring dendritic segments matching the above criteria (control enriched $n = 37$, CA1-KO naive $n = 38$, CA1-KO enriched $n = 41$ and control naive $n = 43$) from age- and sex-balanced sets of 3 animals of each group. These segments represented a total dendritic length of 1001–1284 μm per group of mice.

Data analysis: synapse density. Synapse density was estimated by the disector method[34,35]. From each brain, 15 electron micrographs of separate regions within the stratum radiatum, 100–250 μm from the pyramidal cell layer, were taken from different sections at 10,000× on a JEOL 100C electron microscope to create 15 'reference' planes. The micrographs covered an area of approximately 2100 μm^2 per animal. Micrographs of exactly the same regions were taken on an adjacent section to create 'look-up' planes. The number of synapses contained in a reference plane but absent in the corresponding look-up plane (Q_i) was counted to determine the number of synapses present within the volume defined by the reference plane, the look-up plane and the distance between them (h_i). Two sides of the rectangular picture were assigned randomly as inclusion or exclusion edges to create a counting frame that minimized potential edge effects across samples[41]. To increase the sampling reliability, 606–1043 synapses were counted over a total area of 8,400–14,700 μm^2 from 600 electron micrographs for each experimental group of mice. Section thickness (h_i) was determined by scanning electron microscope measurements (see Histology). Estimated synapse density (est N_v) was calculated as

$$\text{est } N_v = \Sigma Q_i / \Sigma (A_i \times h_i)$$

Note: Additional methods details can be found on the Nature Neuroscience web site (http://neurosci.nature.com/web_specials/).

Acknowledgements

We thank E. Gould for help with stereology and statistics and reading the manuscript, and P. Tanapat for technical advice concerning the Golgi method. This work was supported in part by a postdoctoral fellowship from Fondation pour la Recherche Medicale to C.R. and by grants from Princeton University, Beckman Foundation and NIH to J.Z.T.

RECEIVED 12 OCTOBER; ACCEPTED 28 DECEMBER 1999

1. Rosene, D. L. & Van Hoesen, G. W. in *Cerebral Cortex* Vol. 6: *Further Aspects of Cortical Function, Including Hippocampus* (eds. Jones, E. G. & Petes, A.) 345–447 (Plenum, New York, 1987).
2. Scoville, W. B. & Milner, B. Loss of recent memory after bilateral hippocampal lesion. *J. Neurol. Neurosurg. Psychiatry* **20**, 11–12 (1957).
3. Zola-Morgan, S., Squire, L. R. & Amaral, D. G. Human amnesia and the medial temporal region: enduring memory impairment following a bilateral lesion limited to field CA1 of the hippocampus. *J. Neurosci.* **6**, 2950–2967 (1986).
4. Squire L. R. Memory and the hippocampus: a synthesis from findings with rats, monkeys, and humans. *Psychol. Rev.* **99**, 195–231 (1992).
5. Mumby, D. G. *et al.* Ischemia-induced object-recognition deficits in rats are attenuated by hippocampal ablation before or soon after ischemia. *Behav. Neurosci.* **110**, 266–281 (1996).
6. Wood, E. R., Dudchenko, P. A. & Eichenbaum, H. The global record of memory in hippocampal neuronal activity. *Nature* **397**, 613–616 (1999).
7. Moriyoshi, K. *et al.* Molecular cloning and characterization of the rat NMDA receptor. *Nature* **354**, 31–37 (1991).
8. Nicoll, R. A. & Malenka, R. C. Expression mechanisms underlying NMDA receptor-dependent long-term potentiation. *Ann. NY Acad. Sci.* **868**, 515–525 (1999).
9. Bear, M. F. & Malenka, R. C. Synaptic plasticity: LTP and LTD. *Curr. Opin. Neurobiol.* **4**, 389–399 (1994).
10. Tang, Y.-P. *et al.* Genetic enhancement of learning and memory in mice. *Nature* **401**, 63–69 (1999).
11. Tsien, J. Z. *et al.* Subregion- and cell type-restricted gene knockout in mouse brain. *Cell* **87**, 1317–1326 (1996).
12. Tsien, J. Z., Huerta, P. T. & Tonegawa, S. The essential role of hippocampal CA1 NMDA receptor-dependent synaptic plasticity in spatial memory. *Cell* **87**, 1327–1338 (1996).
13. McHugh, T. J., Blum, K. I., Tsien, J. Z., Tonegawa, S. & Wilson, M. A. Impaired hippocampal representation of space in CA1-specific NMDAR1 knockout mice. *Cell* **87**, 1339–1349 (1996).
14. Woolf, N. J. A structural basis for memory storage in mammals. *Prog. Neurobiol.* **55**, 59–77 (1998).
15. Bailey, C. H. & Kandel, E. R. Structural changes accompanying memory storage. *Annu. Rev. Physiol.* **55**, 397–426 (1993).
16. Moser, M. B., Trommald, M. & Andersen, P. An increase in dendritic spine density on hippocampal CA1 pyramidal cells following spatial learning in adult rats suggests the formation of new synapses. *Proc. Natl. Acad. Sci. USA* **91**, 12673–12675 (1994).
17. Goodman, C. S. & Shatz, C. J. Developmental mechanisms that generate precise patterns of neuronal connectivity. *Cell* **72**, Suppl. 77–98 (1993).
18. Li, Y., Erzurumlu, R. S., Chen, C., Jhaveri, S. & Tonegawa, S. Whisker-related neuronal patterns fail to develop in the trigeminal brainstem nuclei of NMDAR1 knockout mice. *Cell* **76**, 427–437 (1994).
19. Kirov, S. A. & Harris, K. M. Dendrites are more spiny on mature hippocampal neurons when synapses are inactivated. *Nat. Neurosci.* **10**, 878–883 (1999).
20. Sorra, K. E. & Harris, K. M. Stability in synapse number and size at 2 hr after long-term potentiation in hippocampal area CA1. *J. Neurosci.* **18**, 658–671 (1998).
21. Mansuy, I. M., Mayford, M., Jacob, B., Kandel, E. R. & Bach, M. E. Restricted and regulated overexpression reveals calcineurin as a key component in the transition from short-term to long-term memory. *Cell* **92**, 39–49 (1998).
22. Kogan, J. H. *et al.* Spaced training induces normal long-term memory in CREB mutant mice. *Curr. Biol.* **7**, 1–11 (1996).
23. Strupp, B. J. & Levitsky, D. A. Social transmission of food preferences in adult hooded rats (*Rattus norvegicus*). *J. Comp. Psychol.* **98**, 257–266 (1984).
24. Bunsey, M. & Eichenbaum, H. Selective damage to the hippocampal region blocks long-term retention of a natural and nonspatial stimulus-stimulus association. *Hippocampus* **5**, 546–556 (1995).
25. Phillips, R. G. & LeDoux, J. E. Differential contribution of amygdala and hippocampus to cued and contextual fear conditioning. *Behav. Neurosci.* **106**, 274–285 (1992).
26. Kempermann, G., Kuhn, G. H. & Gage, F. H. More hippocampal neurons in adult mice living in an enriched environment. *Nature* **386**, 493–495 (1997).
27. Dalrymple-Alford, J. C. & Benton, D. Preoperative differential housing and dorsal hippocampal lesions in rats. *Behav. Neurosci.* **98**, 23–34 (1984).
28. Rosenzweig, M. R. Environmental complexity, cerebral change, and behavior. *Am. Psychol.* **21**, 321–332 (1966).
29. Diamond, M. C. *Enriching Heredity: The Impact of the Environment on the Anatomy of the Brain* (Free Press, New York, 1988).
30. Fiala, B. A., Joyce, J. N. & Greenough, W. T. Environmental complexity modulates growth of granule cell dendrites in developing but not adult hippocampus of rats. *Exp. Neurol.* **59**, 372–383 (1978).
31. Greenough, W. T., Withers, G. S. & Wallace, C. S. in *The Biology of Memory* (eds. Squire, L. R. & Lindenbaum, E.) 159–185 (Schattauer, Stuttgart, 1990).
32. Gabbott, P. L & Somogyi, J. The "single" Golgi impregnation procedure: methodological description. *J. Neurosci. Methods* **11**, 221–230 (1984).
33. Sorra, K. E., Fiala, J. C. & Harris, K. M. Critical assessment of the involvement of perforations, spinules, and spine branching in hippocampal synapse formation. *J. Comp. Neurol.* **398**, 225–240 (1998).
34. Sterio, D. C. The unbiased estimation of number and sizes of particles using the disector. *J. Microsc.* **134**, 127–136 (1984).
35. DeGroot, D. M. G. & Bierman, E. P. B. A critical evaluation of methods for estimating the numerical density of synapses. *J. Neurosci. Methods* **18**, 79–101 (1986).
36. Gray, E. G. Axosomatic and axodendritic synapses of the cerebral cortex: An electron microscopic study. *J. Anat.* **83**, 420–433 (1959).
37. Nicoll, R. A. & Malenka, R. C. Contrasting properties of two forms of long-term potentiation in the hippocampus. *Nature* **377**, 115–118 (1995).
38. Stevens, C. F. & Sullivan, J. Synaptic plasticity. *Curr. Biol.* **8**, R151–153 (1998).
39. Woolley, C. S., Gould, E., Frankfurt, M. & McEwen, B. S. Naturally occurring fluctuation in dendritic spine density on adult hippocampal pyramidal neurons. *J. Neurosci.* **10**, 4035–4039 (1990).
40. Franklin, K. B. J. & Paxinos, G. The mouse brain in stereotaxic coordinates. (Academic, San Diego, 1997).
41. Gundersen, H. J. G. Notes on the estimation of the numerical density of arbitrary profiles: the edge effect. *J. Microsc.* **111**, 219–223 (1977).